Journal of Science and Engineering Technology, Vol. 10, No. 2, pp.69-80 (2014)

Active Magnetic Bearing System Equipped With a Fuzzy Logic Controller

SENG-CHI CHEN[1], VAN-SUM NGUYEN[2], DINH-KHA LE[2] and NGUYEN THI-HOAI NAM[3]

[1]Department of Electrical Engineering, Southern Taiwan University of Science and Technology

No. 1, Nan-Tai Street, Yungkang Dist., Tainan City 71005, Taiwan R.O.C.

[2]Department of Electrical Engineering, Da-Yeh University

No. 168, University Rd., Dacun, Changhua 51591, Taiwan, R.O.C.

[3]Department of Electrical Engineering, Hue Industrial College

No. 70, Nguyen Hue Rd., Hue City, Vietnam.

ABSTRACT

This paper proposes an intelligent control method for positioning an active magnetic bearing (AMB) system, by using emerging fuzzy logic controller (FLC) approaches. An AMB system depends on controlling the air gap between the stator and the rotor. In practice, no precise mathematical model can be established because the rotor displacement in an AMB system is inherently unstable, and the relationship between the current and electromagnetic force is highly nonlinear. Nearly all industrial applications of AMBs are still based on conventional proportional-integral-derivative or proportional-derivative controllers. Recently, fuzzy logic has been used as a mathematical tool for addressing the uncertainties in human perception and reasoning. It also provides a framework for applying approximate human reasoning capabilities to knowledge-based systems. This study designed a closed-loop decentralized FLC for an AMB system. The control algorithm was numerically evaluated to construct a multiple-input multiple-output mathematical model of the controlled system. The membership functions and rule design of the FLC were based on the mathematical model of an AMB system. The simulation results for the AMB system indicated that the system responded by demonstrating satisfactory control performance without overshoot, maintaining a zero-error steady state, and exhibiting a short rise time. The proposed controller can be feasibly applied to AMB systems exhibiting various external disturbances and the FLC with capacities operates effectively in a wide range of shaft positions.

***Key Words*:** active magnetic bearing (AMB), fuzzy locgic controller (FLC), proportional-integral-derivative (PID).

模糊控制器在主動磁浮軸承系統的應用

陳盛基[1]　阮文森[2]　黎庭軻[2]　阮氏櫰南[3]

[1]南台科技大學電機工程學系

71005 台南市永康區南台街 1 號

[2]大葉大學電機工程學系

51591 彰化縣大村鄉學府路 168 號

[3]順化工業學院電機工程學系

越南順化市阮順化路 70 號

摘 要

本文提出一種智慧型控制方法應用於主動式磁浮軸承系統，此方法利用模糊邏輯控制器進行此磁浮系統的懸浮定位控制，令磁浮軸承之定子與轉子之間維持固定的氣隙。由於磁浮軸承本質上爲不穩定的系統，且通入之電流與磁力之間爲高度非線性，工業界目前仍採用傳統的比例-積分-微分控制器，而模糊邏輯控制器利用近似人類感知與推理的能力，儼然成爲一套解決不確定問題的數學工具，因此本研究針對磁浮軸承系統設計一套閉回路模糊控制器，首先建構磁浮軸承多輸入多輸出之數學模型，再依此模型設計模糊控制器輸出入變數的歸屬函數及規則，模擬結果顯示系統的響應具有滿意的控制性能，無超越量、零穩態誤差及相當短的上升時間，所提的控制器可應用於具外界干擾之磁浮軸承，且轉軸可在寬廣的位置範圍內操作。

關鍵詞：主動磁浮軸承，模糊邏輯控制，比例 – 積分 - 微分。

I. Introduction

Magnetic bearings are electromechanical devices that use magnetic forces to completely levitate a rotor without physical contact. They use magnetic force to suspend the rotor in an air gap. No mechanical contact is made between the rotor and the stator. Because the system does not undergo friction or wear, it requires no lubrication. In addition, magnetic bearings do not produce pollution, they have a long working life, and they can used for a wide range of potential applications in the aerospace, energy, transportation, and other high-technology fields, as well as in high-speed ultraprecision machine tools [10, 17]. This paper presents an AMB system that supports the ventilator rotor to ensure the absence of friction between the rotor and the stator and, therefore, the absence of wear, thereby improving the life of the ventilator and its rate of rotation [4, 5]. The conventional mechanical rotary bearings have several limits in performing the aforementioned task. Because they are in contact with the shaft, friction between the shaft and the bearings occurs. At high rotating speeds, this friction causes the temperature to increase substantially, and results in considerable energy loss. Furthermore, the bearing may be worn or broken. Moreover, designing active controls for magnetic bearing systems is difficult because they are highly nonlinear and exhibit open-loop unstable electromagnetic dynamics. When technology was undeveloped, the main controllers used for AMBs in most practical installations were traditional proportional-integral-derivative(PID)controllers [18, 19]. The performance of the PID controller is generally satisfactory for most practical applications; however, this controller becomes ineffective when the rotor is subjected to extreme operating conditions. Currently, several nonlinear control techniques have been proposed to address the nonlinear dynamics of the AMB. In this study, a method for controlling the position of the actuator using emerging fuzzy logic controller(FLC)approaches was proposed. The FLC has been successfully applied in numerous nonlinear systems in recent years. Moreover, fuzzy control can be used to effectively manage nonlinear and uncertain plants [2, 6-8]. Various fuzzy models and control frameworks have been investigated in numerous studies. The main method is based on adjusting the linear controller signal in a manner that enables nonlinear effects to be effectively compensated. The relationships among attractive forces, electromagnetic currents, and the air gap are described and compensated using fuzzy principles, rather than a precise mathematical-model-based control approach. The results of simulating the AMB system in this study indicate that the system responded by demonstrating satisfactory control performance without overshoot, and exhibited zero steady-state error. This controller also satisfied the requirements of real-time response and stability under disturbances in the control system.

II. Active Magnetic Bearing System Structure and Operating Principles

The system is composed of a ventilator, a rotor shaft, a magnetic bearing, a coupling device, a driving motor, and other components, as shown in Fig.1. Fig.2 presents a technical application of the AMB. For each of the two degrees of freedom, two opposing electromagnets operate in the differential driving mode. In this configuration, the electromagnetic force can be exerted on the rotor in arbitrary directions the *x*-axis or the *y*-axis—to keep the rotor in the central position 14.

In Fig.2, i_0 is the bias current; and i_x and i_y are the control currents along the *x*-axis and *y*-axis, respectively. To elucidate the operating principles of an AMB, the model in Fig.3 of an electromagnet and the main geometrical characteristics of the electromagnet must be considered to calculate the AMB force of a single actuator. The magnetic flux Φ through the stator cross-section A_{fe} is typically assumed to be constant throughout the loop. Furthermore, $A_{fe} = A_\alpha = A$ (where A_α is the cross-section of the air gap *s*) is assumed. Accordingly,

$$\Phi = B_{fe}A_{fe} = B_a A \tag{1}$$

$$B_{fe} = B_a = B \tag{2}$$

The magnetic flux density *B* is given by the following relationship:

$$B = \mu_r \mu_0 H \tag{3}$$

where μ_0 represents the permeability of air ($\mu_0 = 4\pi 10^{-7}$ [H/m]) and μ_r is the relative permeability of the iron core.

The magnetic circuit in Fig.2 is calculated using the following equation

$$\oint Hds = ni \tag{4}$$

$$ni = H_{fe}l_{fe} + 2H_a s \tag{5}$$

where *ds* is the differential length of the flux path; *n* is the number of coil turns on the magnetic actuator; *i* is the total current in the magnet coils, and *s* is the air gap between the stator and the rotor. The average magnetic path length in the laminate is l_{fe}; field intensities H_{fe} and H_a from Eq. (5) can be replaced by Eq. (3). After Eqs. (3) and (5) are solved, the relationship between *B* and the flux density, Eq.(6) is obtained.

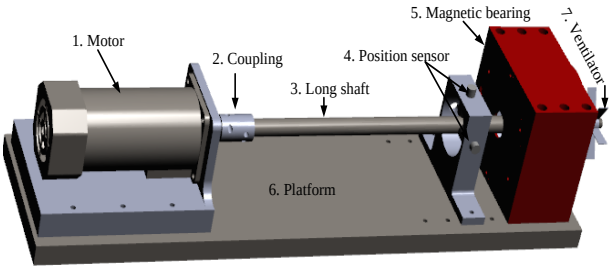

Fig. 1. Architecture of a ventilator AMB system

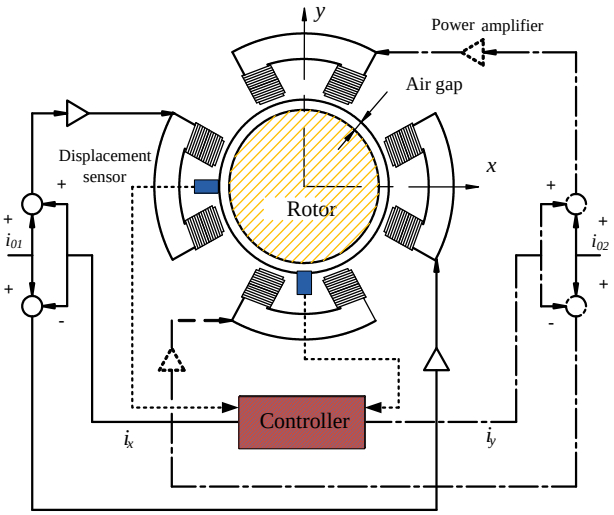

Fig. 2. Current control in differential driving mode

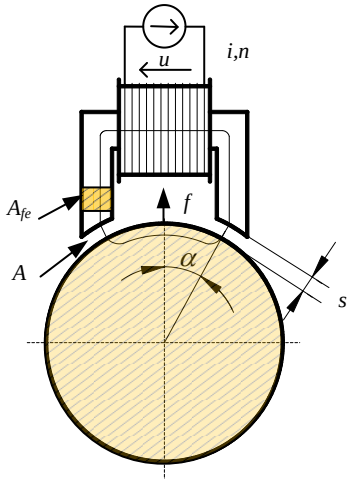

Fig. 3. Magnetic force generated by an AMB

$$B = \mu_0 \frac{ni}{\left(\frac{l_{Fe}}{\mu_r} + 2s\right)} \tag{6}$$

The permeability of iron is μ_r >> 1; consequently, the magnetization of the iron is often neglected. Eq. (6) can then be simplified to

$$B = \mu_0 \frac{ni}{2s} \tag{7}$$

In reference [12], we consider the energy by Eq. (8)

$$W_a = \frac{1}{2} B_a H_a V_a = \frac{1}{2} B_a H_a A_a 2s \tag{8}$$

When the air gap s increases by ds, the $V\alpha$ increases, and energy $W\alpha$ in the field increases by dW. This energy has to be provided mechanically, i.e. an attractive force has to be overcome. Thus, force the partial derivative of the field energy $W\alpha$ with respect to the air gap s, given below:

$$f = \frac{dW_a}{d_s} = B_a H_a A_a = \frac{B^2 A_a}{\mu_0} \tag{9}$$

The angle between the direction of the force and the center of the cross-section A is determined by α (Fig.3). For a common four-pole radial AMB, which has eight actuator teeth, α is 22.5°. Equations (7) and (9) yield the force for one actuator:

$$f = k \frac{i^2}{s^2} \cos\alpha \tag{10}$$

$$k = \frac{1}{4} \mu_0 n^2 A_a \tag{11}$$

III. Mathematical Model of AMB System

A radial AMB consists of two pairs of controlling opposing electromagnets in a differential driving mode, as displayed in Fig.4. Each electromagnet is fed with an operating current with the same bias, and a control current is added to the current that is fed to one magnet and subtracted from the current that is fed to the other magnet, depending on the direction of the desired force. As shown in Fig.4, the force produced by one electromagnet increases while the force produced by the other magnet decreases; consequently, two forces simultaneously act on the rotor. A simplified form of Eq. (10) is presented in the previous section. The air gaps are defined by the deviation x[m] and the nominal air gap s_0 [m]; for the differential driving mode, the variable s is defined as

$$s_+ = s_0 - x \tag{12}$$

$$s_- = s_0 + x \tag{13}$$

where the subscripts "+" and "-" denote the electromagnets that receive the added and subtracted currents, respectively.

The force (f_x) in Fig. 4 represents the difference in the forces between the two magnets. Both of the forces are obtained by inserting the sum (i_0+i_x) and the difference (i_0-i_x) for current i into Eq. (10). To calculate the air gaps, (s_0+x) and (s_0-x) are inserted. The total nonlinear attractive electromagnetic force for the x-axis is modeled as follows:

$$f_x = f_+ - f_- = k\left(\frac{(i_0 + i_x)^2}{(s_0 - x)^2} - \frac{(i_0 - i_x)^2}{(s_0 + x)^2}\right)\cos\alpha \tag{14}$$

Similarly for the y-axis, the attractive electromagnetic force is

$$f_y = f_+ - f_- = k\left(\frac{(i_0 + i_y)^2}{(s_0 - y)^2} - \frac{(i_0 - i_y)^2}{(s_0 + y)^2}\right)\cos\alpha \tag{15}$$

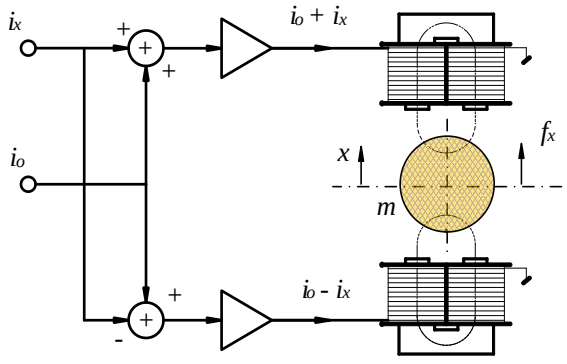

Fig. 4. Pair of electromagnets for magnetic force

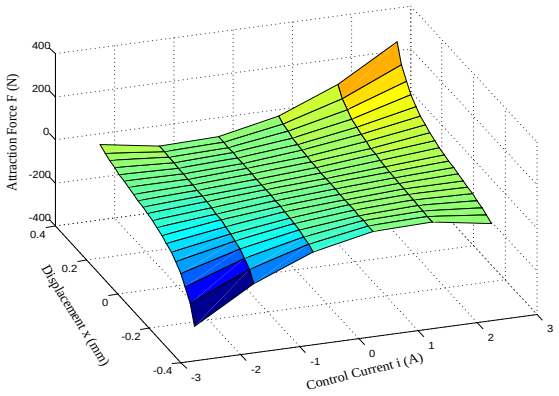

Fig. 5. Characteristics of electromagnetic force.

Figure.5 presents a three-dimensional plot of the magnetic force, which is nonlinearly related to the current and rotor displacement.

The Taylor expansion and linearization of Eqs. (14) and (15) can be obtained from the *x*-axis as follows:

$$k_i = \left.\frac{\partial f_x}{\partial i_x}\right|_{x,\, i_x=0} = \frac{4ki_0}{s_0^{\,2}}, \tag{16}$$

$$k_x = \left.\frac{\partial f_x}{\partial x}\right|_{x,\, i_x=0} = \frac{4ki_0^{\,2}}{s_0^{\,3}} \tag{17}$$

Therefore, the net magnetic force that is exerted by the complimentary pole pairs in a fixed direction is

$$f_x = k_i i_x + k_x x \tag{18}$$

where k_x is the bias stiffness and k_i is the current stiffness. Similarly for the *y*-axis, the magnetic force is

$$f_y = k_i i_y + k_x y \tag{19}$$

The rotor can be regarded as a rigid body. Under the effect of the magnetic levitation force, the equation for calculating rotor motion is

$$m\ddot{x} = f_x + F_d \tag{20}$$

where $\ddot{x}$ represents the acceleration rotation of the rotor; m is the mass of the shaft; and F_d is the disturbing force.

IV. Dynamic Model of an AMB System

1. Interference of two perpendicular axes in a magnetic bearing

During the operation of an AMB system, the generated radial forces are aligned on two perpendicular axes, which typically coincide with the *x*- and *y*-axis displacements. However, radial force misalignment (i.e., when the radial forces are not aligned with the *x*- and *y*-axes) can occur for several reasons. Assuming that an electromagnet of a radial magnetic bearing is constructed with a misalignment at an angle with respect to the radial displacement sensors, the direction of the generated radial force exhibits an angular position error, which results in the interference of *x*- and y-axis force components. The interference between the *x*- and *y*-axis radial forces can cause critical problems. In this section, radial interference and its influence on the feedback system are examined [9].

Figure.6 shows two the perpendicular *x*- and *y*-axes and the feedback radial forces, F_{rfx} and F_{rfy}, with a slightly delayed angular position. The rotor is rotating in a counterclockwise direction. The direction angle error is defined as φ_{ae} and the interference radial forces can be written as follows:

$$f_{irfx} = \sin\varphi_{ae} F_{rfx} \tag{21}$$

$$f_{irfy} = -\sin\varphi_{ae} F_{rfy} \tag{22}$$

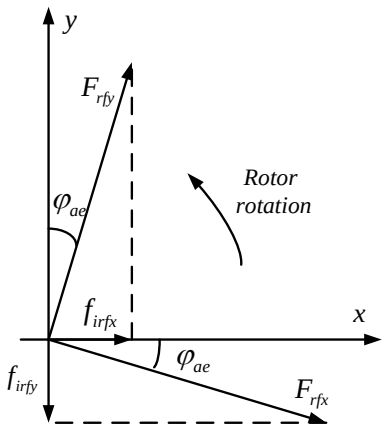

Fig. 6. Angular position error

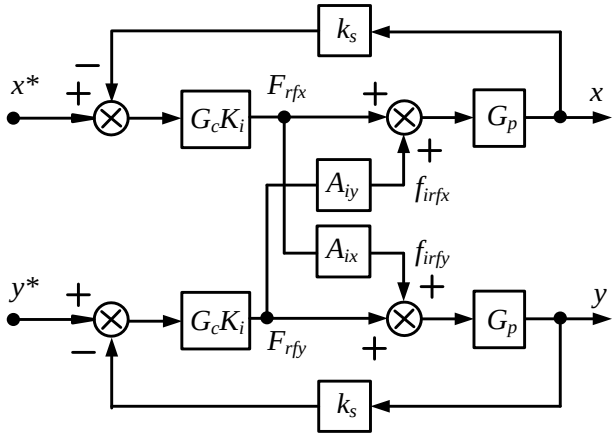

Fig. 7. Diagram interference in two-axes of AMB system

Figure.7 shows a block diagram that depicts the interference of the two *x*-axes and *y*-axes. The outputs are the radial positions and the inputs are the references. The upper and lower blocks are the components of the *x*-axis and *y*-axis dynamic models, respectively. The interference is generated by $-\sin\varphi_{ae}$ and $\sin\varphi_{ae}$. The decrease in radial force caused by $\cos\varphi_{ae}$ is disregarded because φ_{ae} is small.

2. Radial force interference of two axes in an AMB system

The radial force on the *y*-axis is written as $k_x y$, where k_x is the force-displacement factor and y is the *y*-axes shaft displacem-ent. The displacement-originated moment M_{xd} around the *x*-axis and the moment M_{xd} around the *y*-axis are written as Eqs. (23) and (24) , respectively:

$$M_{xd} = -k_x y l_{rt} \tag{23}$$

$$M_{yd} = k_x x l_{rt} \tag{24}$$

The sum of the moments around the *x*-axis and *y*-axis are given as

$$M_x = -\frac{mgh}{l_{rt}} y - F_y l_{rt} - k_x l_{rt} y \tag{25}$$

$$M_y = \frac{mgh}{l_{rt}} x + F_x l_{rt} + k_x l_{rt} x \tag{26}$$

The dynamic motion equations for an AMB system can be expressed as follows:

$$\ddot{y} = -\chi\dot{x} + \gamma y + \rho F_y \tag{27}$$

$$\ddot{x} = -\chi\dot{y} + \gamma x + \rho F_x \tag{28}$$

$$\chi = \frac{\Omega_{rm} I_k}{I_i} \tag{29}$$

$$\gamma = \frac{mgh + k_x l_{rt}^2}{I_i} \tag{30}$$

$$\rho = \frac{l_{rt}^2}{I_i} \tag{31}$$

where l_{rt} is the length from the coupling to the rotor center; h is the height of the center gravity belonging to a magnetic bearing; F_x and F_y are the current-driven radial forces generated in the magnetic bearing on the *x*- and *y*-axes, respectively; x and y are the displacement of the *x*- and *y*-axes, respectively; I_i and I_k are the moments along the *i*- and *k*-axes; and Ω_{rm} is the rotational speed of the rotor.

The dynamics of the two axes in an AMB system are shown in Fig.8. The inputs are the suspension radial forces F_x and F_y and the outputs are the *x*- and *y*-axis shaft displacements. Cross-coupling blocks are caused by gyroscopic effects and positive feedback loops are caused by the weight and the force-displacement factor.

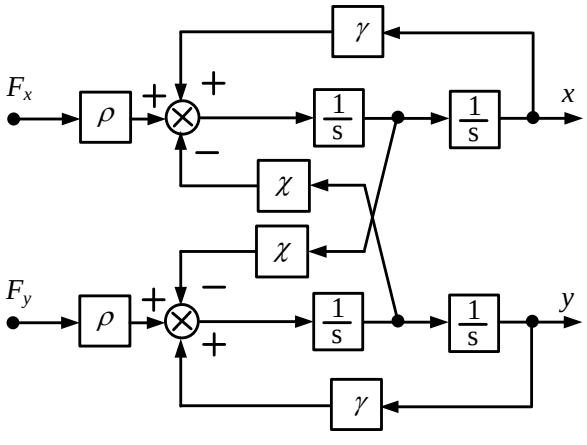

Fig. 8. Radial force and displacement blocks

V. Control System Design

1. Fuzzy Inference Systems

The fuzzy inference system (FIS) is a commonly used computing framework based on the concepts of fuzzy set theory, fuzzy if-then rules, and fuzzy reasoning [1, 11, 12]. Currently, the FIS has been applied in various fields such as automatic control systems, robotics, and 3-D animation systems, and has been used in analyzing a power system and identifying harmonic disturbance problems, controlling heating and cooling in commercial appliances, conserving energy, and enabling effective operation. The FIS can be referred to as a fuzzy-rules-based system, a fuzzy expert system, a fuzzy model, fuzzy associative memory, or, simply, as a fuzzy system. The basic structure of an FIS consists of four conceptual components, as shown in Fig. 9.

Fuzzification refers to the transformation of the crisp inputs into degrees of match with linguistic values. The crisp inputs are converted to linguistic variables in the fuzzification process based on membership functions (MFs). The knowledge base consists of a rule base and a database. The rule base contains a number of fuzzy if-then rules, and the database defines the MFs of the fuzzy sets used in the fuzzy rules. The fuzzy inference engine performs inference operations on the rules. Defuzzification refers to converting the fuzzy results of the FIS into a crisp output, as shown in Fig. 9. The knowledge base provides MFs and fuzzy rules required to execute the process. Crisp variables are the inputs of the system. These variables are converted to linguistic variables at the fuzzification stage and then become the fuzzy input used in the fuzzy inference engine. These fuzzy inputs can be changed to fuzzy output using the rules of the fuzzy inference engine. The fuzzy output subsequently becomes the crisp output of the system after passing through the defuzzification stage. Depending on the type of fuzzy reasoning and the fuzzy if-then rules employed, an FIS can be classified into three types: the Tsukamoto-type FIS, Mamdani-type FIS, and Takagi-Sugeno-type FIS. An in-depth analysis of each of these FISs is described in [3, 13, 15, 16,].

2. Fuzzy logic controller design

Figure 10 shows the synoptic scheme of the fuzzy controller, which possesses two inputs, the error (*e*) and the derivative of the error (*de*), and output (*u*). The basis of the FLC is the representation of linguistic descriptions as MFs.

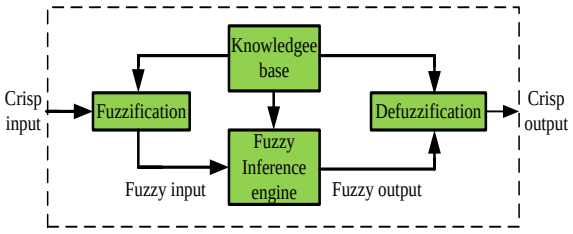

Fig. 9. The basic components of fuzzy inference system

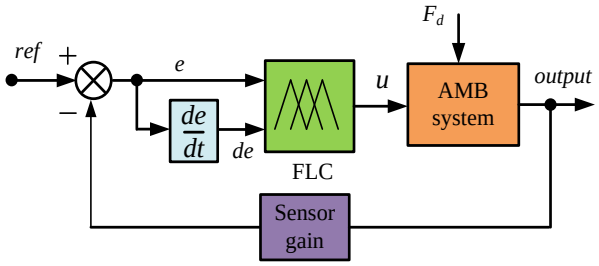

Fig. 10. Fuzzy logic controller synoptic diagram

The MF indicates the degree to which a value belongs to the class labeled by linguistic description. In FLC algorithms, the degree of membership serves as the input. Determining the appropriate degree of membership is a component of the design process. Once the MFs are defined, the input values are transformed into a degree of an MF with the linguistic descriptor values varying from 0 to 1. This process is called fuzzification. The resulting fuzzified data are passed through an inference mechanism that contains the output rules. After the rules are applied, the combined effect of all of the rules is evaluated according to the proper weightage for each rule. The weightage is generally used to fine-tune the fuzzy controller, and this process is called defuzzification.

In this study, two inputs (*e*) and (de) and a single output (*u*) were defined for the system. The linguistic levels of these inputs were designated as *N*: negative; *Z*: zero; and *N*: negative. Fuzzy logic was characterized by three fuzzy sets (*N*, *Z*, *P*) for inputs (*e*) and (*de*). The linguistic levels of these outputs were designated as *BN*: big negative; *SN*: small negative; *ZE*: zero; *SP*: small positive; and *BP*: big positive. Fuzzy logic was characterized by five fuzzy sets (*BN*, *SN*, *ZE*, *SP*, *BP*) for the output (*u*) variable. A Gaussian MF was employed as the inputs, and a triangular MF was employed as the output fuzzy sets of the FLC. The MFs are shown in Figs. 11 and 12. Implication using a Takagi-Sugeno-type FIS we chose aggregation is Max-

Min, and defuzzification was performed using the centroid technique.

The control rules of the fuzzy controllers were a set of heuristically selected fuzzy rules. The processing time required when using an FLC depends upon the number of rules that must be evaluated. Large systems containing numerous rules require extremely powerful and fast processors to perform computations in real time. The fuzzy controller rule base was composed of 9 rules for the output (*u*) variable, as shown in Table 1.

The rule viewer and the control surfaces of FLC are shown in Figs.13 and 14, respectively.

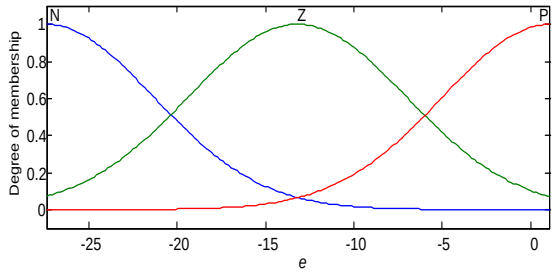

Fig. 11. Membership functions of input *e*

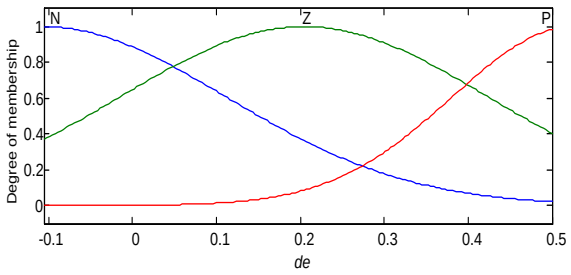

Fig. 12. Membership functions of input *de*

Table 1. Rules base of FLC

u		*e*		
		N	***Z***	***P***
de	***N***	BP	SP	BN
	Z	BN	ZE	SN
	P	ZE	SN	BP

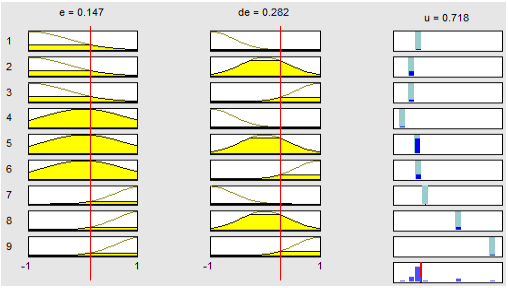

Fig. 13. Rule viewer of fuzzy

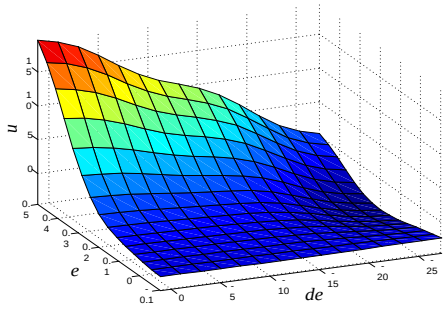

Fig. 14. Relationship between *e*, *de*, *u*

VI. Simulation Results

The results of performing simulations using FLC methodologies were derived using MATLAB-Simulink for an AMB system, as shown in Figs. 15 to 19. The step responses of rotor displacement from the gap sensor in an AMB system using the FLC are shown in this figure. Table 2 presents the parameters of the AMB system.

As shown in Fig.15, the reference signal *x** and *y** was compared with the position of the sensor on the *x*-axis and *y*-axis, respectively. The signal was used as the input for the FLC, which generated a control effort according to the measurements using current amplifiers. The control signals were transformed into magnetic forces by four actuating magnets around the rotor, which held the rotor at the reference positions. In this simulation, the goal was to control the position of the rotor with respect to the center of the stator. After the simulation was conducted, the performance characteristics were observed on the respective scopes. The response curves of rotor displacement, current, and disturbing force were observed and are shown in Figs.20–23, respectively. The simulation results shown in Figs.20 and 21 indicate that the operating envelope of the rotor displacement covered the entire feasible region (up to 0.5 mm), and the current response in the system was stable and balanced. The simulation results for the PID controller and FLC

are shown in Fig.22. These results clearly indicate that the system was a typical nonlinear unstable system, and the rotor air gap was small; consequently, using the traditional standard PID control parameters caused a large overshoot, a long settling time, and a slow response. When the system undergoes a large disturbance (Fig.23), it is prone to collisions between the stator and rotor, causing serious damage to the system. The FLC provides a more favorable response than the PID controller does. This demonstrates that the FLC remarkably reduced the overshoot and settling time, and produced a small overshoot and a small steady-state error when an external disturbance occurred. The FLC achieved favorable performance levels in both the transient and steady-state periods.

Table 2. The parameters of an AMB system

1	Mass of shaft (m)	2.72kg
2	Number of coil turns (n)	120
3	Resistance of the coil (R)	8.5Ω
4	Inductance of an axial coil (L)	19.2mH
5	Permeability of air (μ_0)	$4\pi\times10^{-7}$ H /m
6	Nominal air gap length (s_0)	0.5mm
7	Bias currents to be used (i_{bias})	1.5A
8	Force displacement factor (K_x)	342478 N /m
9	Force current factor (K_i)	171 N/A
10	Maximum voltage (u_p)	24 V

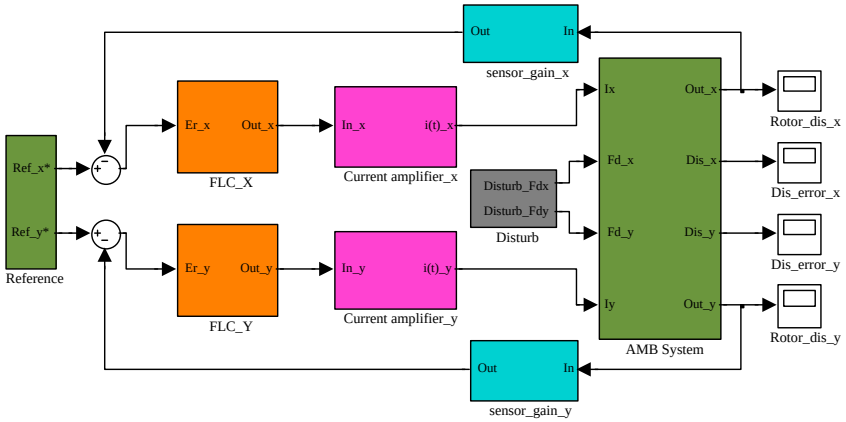

Fig. 15. Matlab-Simulink model for an AMB system.

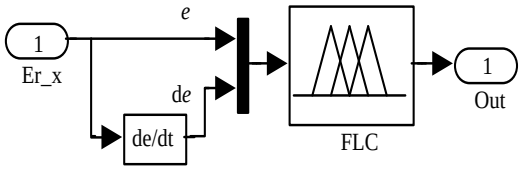

Fig. 16. Block diagram of fuzzy logic controller

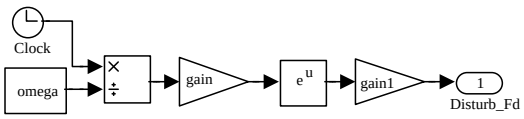

Fig. 18. Block diagram of external disturbances

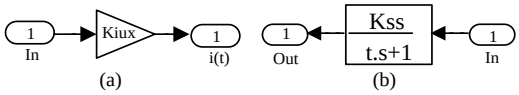

Fig. 17. Current amplifier (a)and position sensor (b)

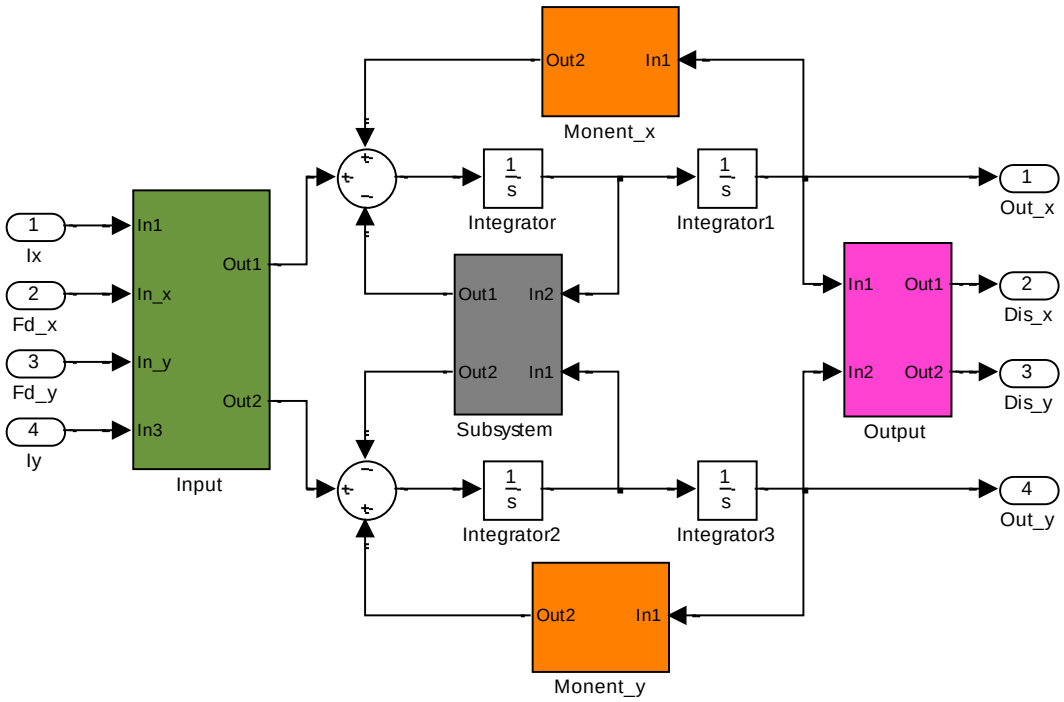

Fig. 19. Block diagram of an AMB System

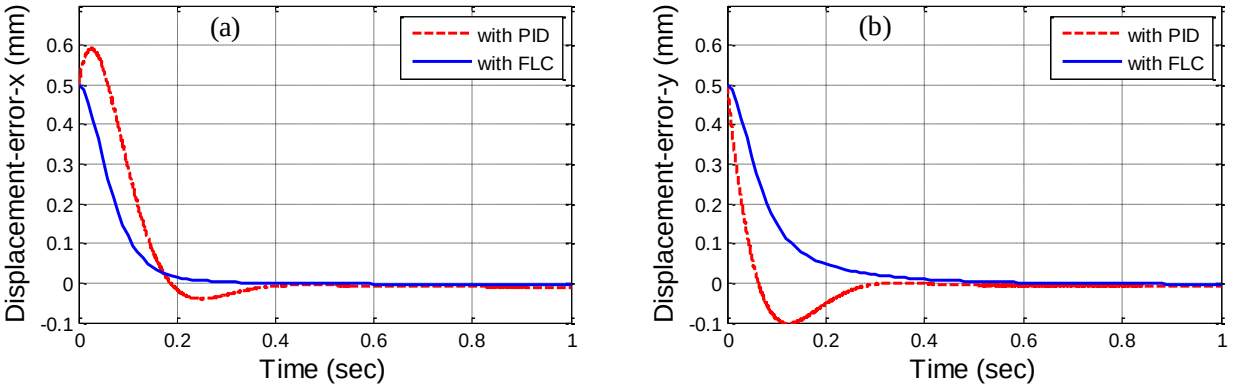

Fig. 20. Displacement error *x*-axis (a) and *y*-axis (b).

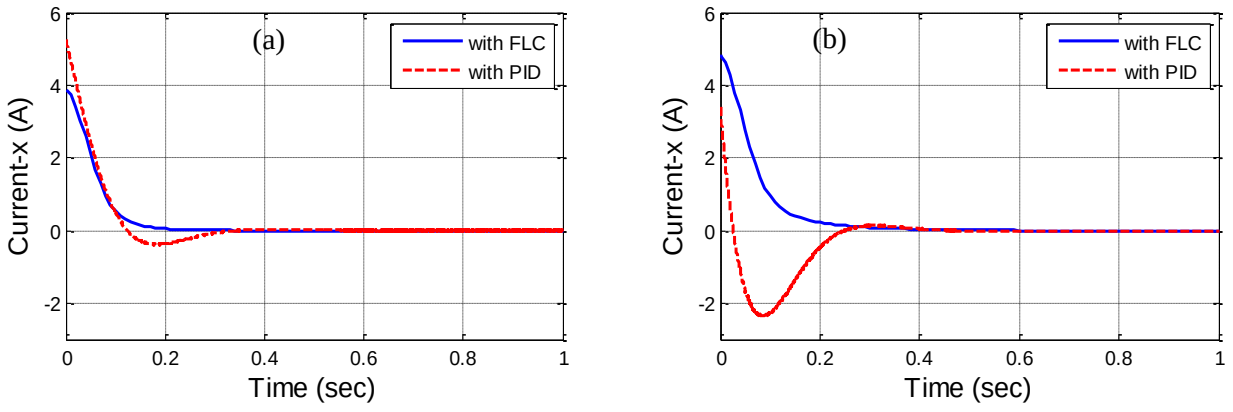

Fig. 21. Current response in an ABM system with *x*-axis (a) and *y*-axis (b).

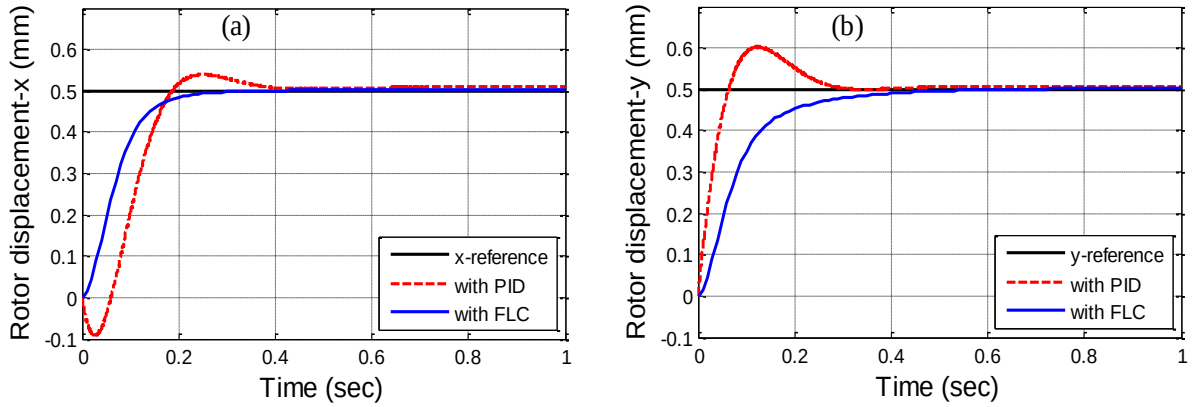

Fig. 22. Step response of rotor position with PID and FLC of *x*-axis (a) and *y*-axis (b)

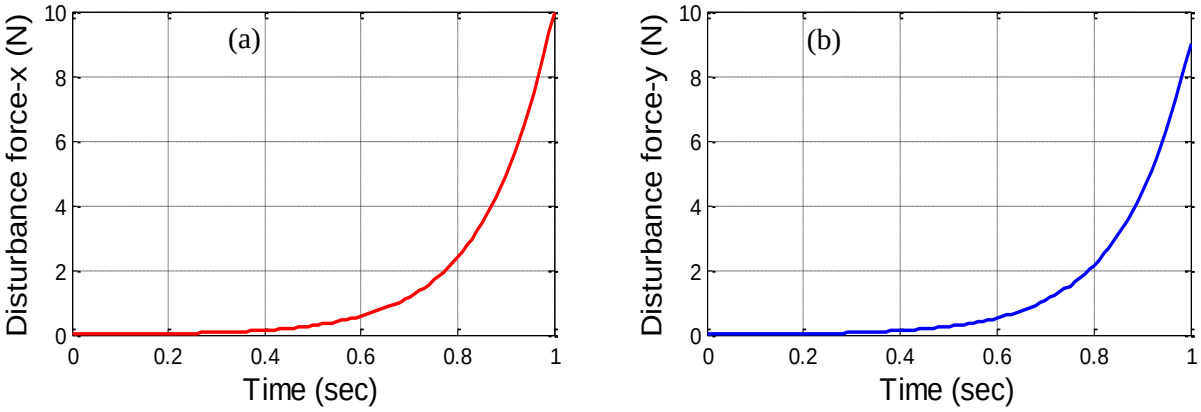

Fig. 23. External disturbance force of *x*-axis (a) and *y*-axis (b)

VII. Conclusions

This study revealed the promising dynamics of the rotor response produced in an AMB system. The FLC was developed for a highly unstable AMB system and tested by conducting simulations using MATLAB software. This controller was used to levitate and stabilize the rotor shaft in the center position of the magnetic bearings and to dampen the shaft vibration with unbalanced forces. The proposed method can also be used to improve the control performance of nonlinear systems. The simulation results indicate that the controller responded favorably to a reference signal. Furthermore, it substantially reduced the overshoot, shortened the adjustment time, accelerated the response, and improved the robustness as well as the dynamic and static performance of the system. The proposed control method can also be effectively used for AMB and other nonlinear systems. The FLC can serve as a simple alternative to traditional controllers used in AMB systems.

References

1. Agarwal, P. K. and S. Chand (2010) Fuzzy logic control of four-pole active magnetic bearing system. The 2010 International Conference on Modelling, Identification and Control (ICMIC), Okayama, Japan.
2. Ajami, A., N. Taheri. and M. Younesi (2009) A novel hybrid fuzzy/LQR damping oscillations controller using STATCOM. Second International Conference on Computer and Electrical Engineering (ICCEE), Dubai, India.
3. Amer, A. F., E. A. Sallam. and W. M. Elawady (2010) Fuzzy pre-compensated fuzzy self-tuning fuzzy PID controller of 3 DOF planar robot manipulators. 2010 IEEE/ASME International Conference on Advanced Intelligent Mechatronics (AIM), Montreal, Canada.
4. Budig, P. K. (2010) Magnetic bearings and some new applications. 2010 XIX International conference on Electrical Machines (ICEM), Rome, Italy.

5. Budig, P. K. (2012) Article to the theory and application of magnetic bearings. 2012 International Symposium on Power Electronics, Electrical Drives, Automation and Motion (SPEEDAM), Sorrento, Italy.
6. Chen, S. C., L. Y. Jyh., V. S. Nguyen. and M. M. Hsu (2013) A novel fuzzy neural network controller for maglev system with controlled-PM electromagnets. *Lecture Notes in Electrical Engineering*, 234, 551-561.
7. Chen, S. C., V. S. Nguyen. and G. Chang (2012) Application of self-tuning fuzzy PID controller on magnetic levitation system. The 11th Taiwan Power Electronics Conference & Exhibition, National Tsing Hua University, Hsinchu, Taiwan.
8. Chen, S. C. and P. C. Tung (2000) Application of a rule self-regulating fuzzy controller for robotic deburring on unknown contours. *Fuzzy Sets and Systems*, 110(3), 341-350.
9. Chiba, A., T. Fukao, O. Ichikawa., M. Oshima., M. Takemoto. and D. G. Dorrell (2005) *Magnetic bearing and bearingless drivers*. Newnes An imprint of Elsevier, Oxford, U.K.
10. Choi, H., G. Buckner. and N. Gibson (2006) Neural robust control of a high-speed flexible rotor supported on active magnetic bearings. American Control Conference, IEEE, Minneapolis, U.S.A.
11. Jang, J. S. R. (1993) ANFIS: adaptive-network-based fuzzy inference system. *IEEE Transactions on Systems, Man and Cybernetics*, 23(3), 665-685.
12. Jang, J. S. R. and C. T. Sun (1995) Neuro-Fuzzy modeling and control. *Proceeding of the IEEE*, 83(3), 378-406.
13. Kwanchai, S., P. Watcharin. and P. Pornjit (2011) A hybrid of fuzzy and fuzzy self-tuning PID controller for servoeElectro-hydraulic system. 2011 6th IEEE Conference on Industrial Electronics and Applications (ICIEA), Beijing, China.
14. Schweitzer G., H. Bleuler. and A. Traxler (1994) *Active Magnetic Bearings*. vdf Hochschulverlag AG, Zurich, Switzerland.
15. Tung, W. L. and C. Quek (2009) A mamdani-takagi-sugeno based linguistic neural-fuzzy inference system for improved interpretability-accuracy representation. IEEE International Conference on Fuzzy Systems, Jeju, Island.
16. Wang, N., C. F. Hu and W. Shi (2012) A mamdani fuzzy modeling method via evolution-objective cluster analysis. 2012 31st Chinese Control Conference (CCC), Hefei, China.
17. Zhang, K., X. Dai. and X. Z. Zhang (2010) Dynamic analysis and control of an energy storage flywheel rotor with active magnetic bearings. 2010 International Conference on Digital Manufacturing and Automation (ICDMA), Changsha, China.
18. Zhang, W. W. (2010) A flywheel energy storage system suspended by active magnetic bearings with fuzzy PID controller. 2010 International Conference on Computer Application and System Modeling (ICCASM), Taiyuan, China.
19. Zhang, W. W. and Y. F. Hu (2009) A prototype of flywheel energy storage system suspended by active magnetic bearings with PID controller. 2009 Asia-Pacific Power and Energy Engineering Conference , Wuhan, China.

收件：102.10.15　修正：102.11.21　接受：103.03.27